Available on CMS information server **CMS IN-2009/007**

CMS Internal Note

The content of this note is intended for CMS internal use and distribution only

31 January 2009

Study of Impact of HO on Jet Reconstruction

Sarah Eno, Dinko Ferencek

University of Maryland, College Park, MD, USA

Abstract

A study of impact of HO on jet reconstruction with the CMS detector is presented. For this purpose a sample of full simulation single-jet events has been produced and analyzed. At the focus of the study was the jet transverse energy resolution. The study shows that inclusion of HO in jet reconstruction leads to small improvements in jet transverse energy resolution and reduces the effects of energy leakage, especially in the most central η region where Ring 0 is located. However, overall improvement in jet transverse energy resolution is relatively small and it does not exceed 1%.

1 Introduction

The hadron outer (HO) calorimeter [1] is the outermost component of the CMS hadronic calorimeter (HCAL) and is located outside the magnet coil. Its primary purpose is to increase the effective thickness of the hadronic calorimeter in the barrel region ($|\eta| < 1.3$) and thus to identify late starting showers leaking outside the hadron barrel calorimeter (HB) and sample their energy. This "tail-catching" property of HO should improve the overall hermetic design of the CMS detector and reduce the tails in the energy resolution function, thus leading to more accurate measurements of the jet transverse energy, E_{T}, and of the missing transverse energy, $\not\!\!E_{\mathrm{T}}$.

The HO design is constrained by the geometry of the muon system. HO covers the region $|\eta| < 1.26$ and consists of five separate rings (0,±1,±2). The central ring (Ring 0) has two scintillator layers on either side of the iron absorber while all other rings have only one scintillator layer on the outer side of the iron absorber. The position of HO scintillator layers in the overall CMS design is shown in Fig. 1. HO scintillators follow the HB tower geometry in η and ϕ. Approximate dimensions along η of different HO rings are given in Table 1.

Table 1: Approximate dimensions along η of different HO rings.

Ring	Dimension along η
0	$\lvert\eta\rvert \lesssim 0.33$
±1	$0.33 \lesssim \lvert\eta\rvert \lesssim 0.86$
±2	$0.86 \lesssim \lvert\eta\rvert \lesssim 1.26$

With the release of `IDEAL_V9` global tag for conditions data [2], HO went from the least noisy HCAL subdetector to the noisiest HCAL subdetector. This prompted its removal from the default jet reconstruction sequence starting from CMSSW_2_1_8 [3]. This, however, might have some unwanted consequences on the reconstruction of jets and missing transverse energy such as reduced energy resolution.

This note is organized as follows. Simulated data as well as jet selection criteria used in this study are described in Section 2. Analysis procedure and obtained results are presented in Section 3. Finally, short summary and conclusions are given in Section 4.

2 Monte Carlo Samples

A sample of full simulation single-jet events was generated using CMSSW_2_1_8 and PYTHIA version 6.416 in particle gun mode. Generated jets were originating from the initial d-quark generated with the transverse momenta of $p_{\mathrm{T}} = 50$, 100, 300, 500, 1000, 2000, 4000, and 7000 GeV/c and with pseudorapidities of $\eta = 0.1$, 0.5, and 1.0. η values were chosen so that most of the HO energy would come from only one HO ring. 6 000 events were generated for each pair of values of transverse momentum p_{T} and pseudorapidity η, i.e., 144 000 events in total. `IDEAL_V9` global tag for conditions data was used.

In order to study the impact of HO on jet reconstruction, `iterativeCone5` jet algorithm was used to reconstruct both generator level jets (GenJets) and calorimeter level jets (calojets). `iterativeCone5` calojets were reconstructed with HO contribution (CaloJetsWithHO) and without HO contribution (CaloJets) included in the jet reconstruction. HO threshold used in calorimeter tower (CaloTower) reconstruction was changed from its default Scheme B [4] value of 1.1 GeV to 2.2 GeV. Reason for this increase in threshold is higher level of noise in HO

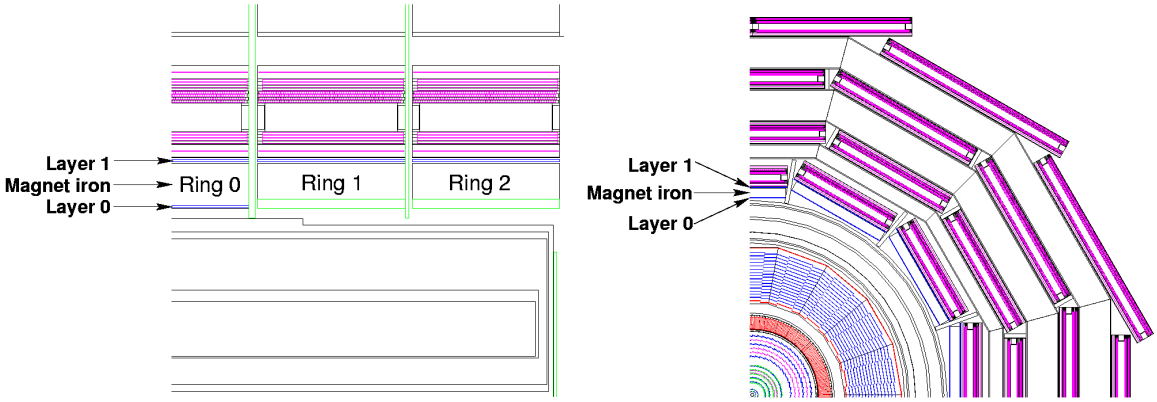

Figure 1: Longitudinal and transverse views of the CMS detector showing the position of HO scintillator layers.

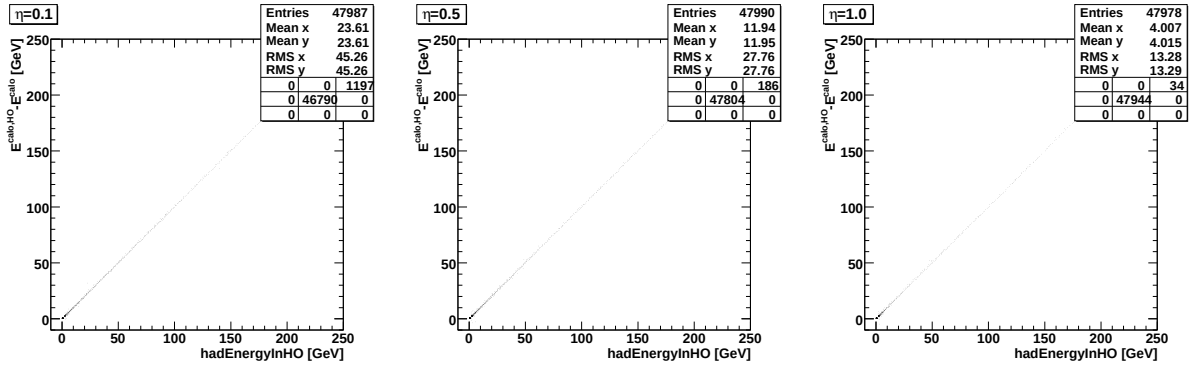

Figure 2: Difference between CaloJetWithHO energy and CaloJet energy ($E^{\text{calo, HO}} - E^{\text{calo}}$) in the same event vs. HO energy contribution (`hadEnergyInHO`) taken from CaloJetWithHO for parton $\eta = 0.1$ (left), 0.5 (center), and 1.0 (right).

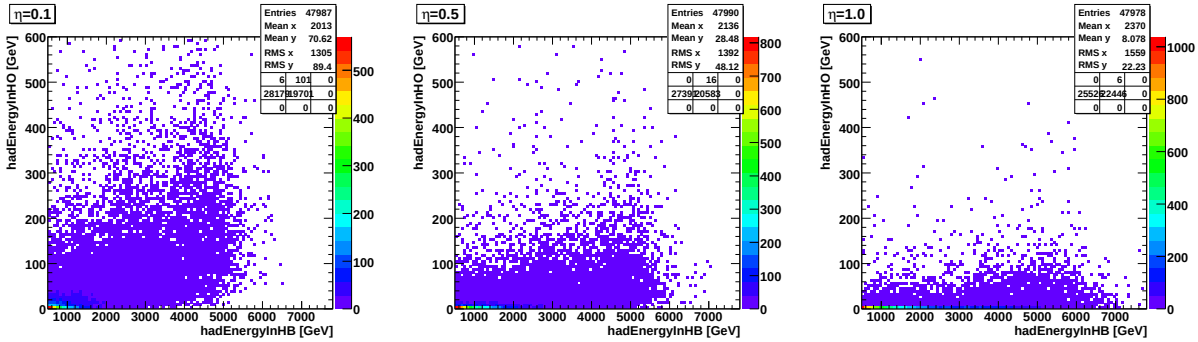

Figure 3: Correlation between HO and HB energy contributions for CaloJetsWithHO for parton $\eta = 0.1$ (left), 0.5 (center), and 1.0 (right).

introduced with `IDEAL_V9` detector conditions for which default Scheme B threshold was not optimized [5]. Additional effect that had to be corrected for is the ECAL cell saturation bug [6] for which only a partial fix was available at the time of writing this note.

2.1 Jet Selection Criteria

In this particular analysis there is exactly one generated GenJet per event and the only selection criterion required was that GenJets have $p_{\text{T}} > 30$ GeV/c. Similarly, for calojets the only selection criterion was that they have $p_{\text{T}} > 15$ GeV/c. After GenJets and calojets had been selected, they were matched using One-To-One matching tool [7]. Some of the obtained kinematic distributions for GenJets and calojets are given in Appendix A. p_{T} spectra of the GenJet constituent particles are given in Appendix B.

3 Results

As it was already mentioned, `iterativeCone5` calojets were reconstructed with and without HO contribution included. It is then expected that the difference between CaloJetWithHO energy ($E^{\text{calo, HO}}$) and CaloJet energy (E^{calo}) in the same event would almost entirely come from the HO energy contribution. This is confirmed in Fig. 2 where a clear correlation between the calojet energy difference ($E^{\text{calo, HO}} - E^{\text{calo}}$) and HO energy contribution (`hadEnergyInHO`) taken from CaloJetWithHO can be observed. Correlation between HO and HB energy contributions for CaloJetsWithHO for different values of parton η is shown in Fig. 3. As expected, correlation is stronger for lower values of η where the effective thickness of HB is smaller.

Distributions from which all results were derived are $E_{\text{T}}^{\text{calo}}/E_{\text{T}}^{\text{gen}}$ and $E_{\text{T}}^{\text{calo, HO}}/E_{\text{T}}^{\text{gen}}$ distributions where $E_{\text{T}}^{\text{calo}}$ ($E_{\text{T}}^{\text{calo, HO}}$) and $E_{\text{T}}^{\text{gen}}$ are transverse energies of the matched CaloJet (CaloJetWithHO) and GenJet, respectively. Obtained $E_{\text{T}}^{\text{calo}}/E_{\text{T}}^{\text{gen}}$ and $E_{\text{T}}^{\text{calo, HO}}/E_{\text{T}}^{\text{gen}}$ distributions for different values of parton η are shown in Figures 4, 5, and 6. As the $E_{\text{T}}^{\text{gen}}$ increases, $E_{\text{T}}^{\text{calo}}/E_{\text{T}}^{\text{gen}}$ ($E_{\text{T}}^{\text{calo, HO}}/E_{\text{T}}^{\text{gen}}$) distributions move to the right and their mean values get closer to 1, as expected. However, for $E_{\text{T}}^{\text{gen}} \gtrsim 2$ TeV mean values of the distributions start to decrease which is

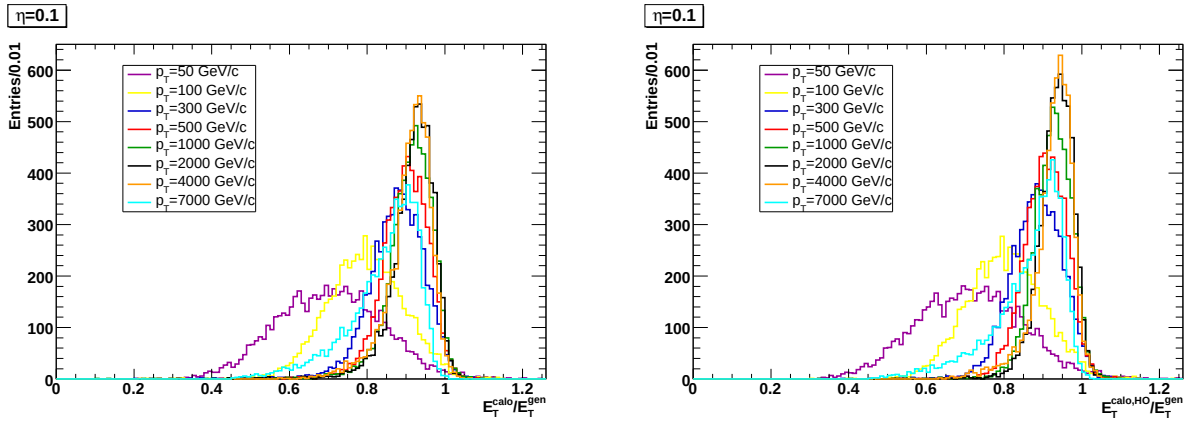

Figure 4: $E_{\mathrm{T}}^{\mathrm{calo}}/E_{\mathrm{T}}^{\mathrm{gen}}$ (left) and $E_{\mathrm{T}}^{\mathrm{calo,\ HO}}/E_{\mathrm{T}}^{\mathrm{gen}}$ (right) distributions for parton $\eta = 0.1$.

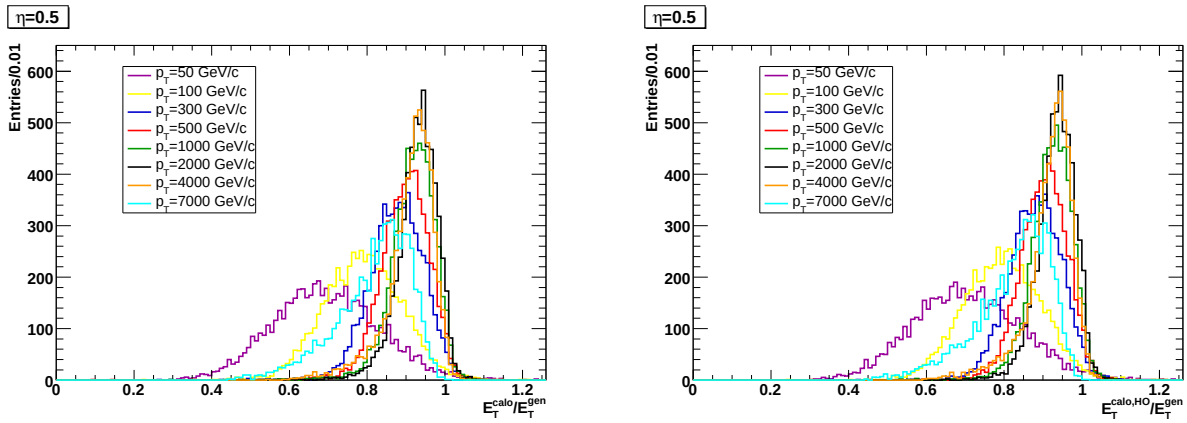

Figure 5: $E_{\mathrm{T}}^{\mathrm{calo}}/E_{\mathrm{T}}^{\mathrm{gen}}$ (left) and $E_{\mathrm{T}}^{\mathrm{calo,\ HO}}/E_{\mathrm{T}}^{\mathrm{gen}}$ (right) distributions for parton $\eta = 0.5$.

due to the fact that saturated ECAL cells even after correction still contain too little energy.

Quantity through which calojets with and without HO were compared is the jet E_{T} resolution. Jet E_{T} resolution is defined as

$$\text{Jet } E_{\mathrm{T}} \text{ resolution} = \frac{\sigma\left(E_{\mathrm{T}}^{\mathrm{calo}}/E_{\mathrm{T}}^{\mathrm{gen}}\right)}{< E_{\mathrm{T}}^{\mathrm{calo}}/E_{\mathrm{T}}^{\mathrm{gen}} >}, \tag{1}$$

where $\sigma\left(E_{\mathrm{T}}^{\mathrm{calo}}/E_{\mathrm{T}}^{\mathrm{gen}}\right)$ and $< E_{\mathrm{T}}^{\mathrm{calo}}/E_{\mathrm{T}}^{\mathrm{gen}} >$ are the standard deviation and the mean, respectively, of the Gaussian fit to $E_{\mathrm{T}}^{\mathrm{calo}}/E_{\mathrm{T}}^{\mathrm{gen}}$ distribution in 2σ region around the peak of the distribution. A full set of Gaussian fits to distributions shown in Figures 4, 5, and 6 is given in Appendix C. By combining results from these fits, jet E_{T} resolution as a function of GenJet transverse energy $E_{\mathrm{T}}^{\mathrm{gen}}$ was obtained and is shown in Figures 7, 8, and 9 for different values of parton η. From these plots it can be noticed that for calojets with HO contribution included, energy resolution gets slightly improved, most notably for very high energy jets in Ring 0. However, overall improvement is still relatively small and it does not exceed 1%. For $E_{\mathrm{T}}^{\mathrm{gen}} \gtrsim 2$ TeV, energy resolution starts to degrade due to ECAL cell saturation bug.

Effect of energy leakage outside the HB can be studied by looking at the fraction of events with $E_{\mathrm{T}}^{\mathrm{calo}}/E_{\mathrm{T}}^{\mathrm{gen}}$ ($E_{\mathrm{T}}^{\mathrm{calo,\ HO}}/E_{\mathrm{T}}^{\mathrm{gen}}$) more than 3σ below the mean value. First thing to notice in Figure 10 is that any result for $E_{\mathrm{T}}^{\mathrm{gen}} \gtrsim 2$ TeV has to be discarded due to ECAL cell saturation bug. However, for $E_{\mathrm{T}}^{\mathrm{gen}} \lesssim 2$ TeV it can be seen that with HO included the fraction of events with significant leakage is kept below $\sim 1.5\%$. Improvement is most significant for Ring 0 while for Ring 2 it practically vanishes.

Effect of adding HO energy contribution (`hadEnergyInHO`) with different weight factors on jet E_{T} resolution is illustrated in Appendix D.

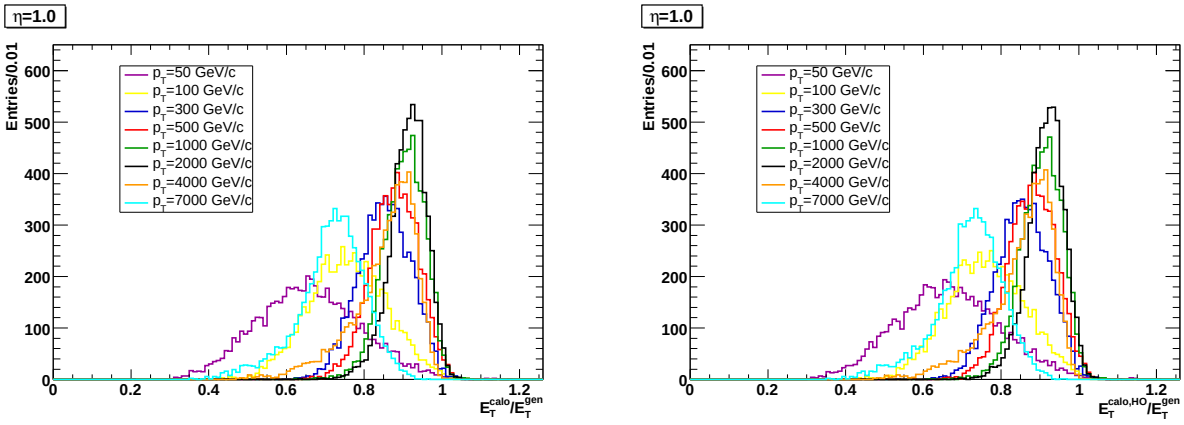

Figure 6: $E_{\mathrm{T}}^{\mathrm{calo}}/E_{\mathrm{T}}^{\mathrm{gen}}$ (left) and $E_{\mathrm{T}}^{\mathrm{calo,\ HO}}/E_{\mathrm{T}}^{\mathrm{gen}}$ (right) distributions for parton $\eta = 1.0$.

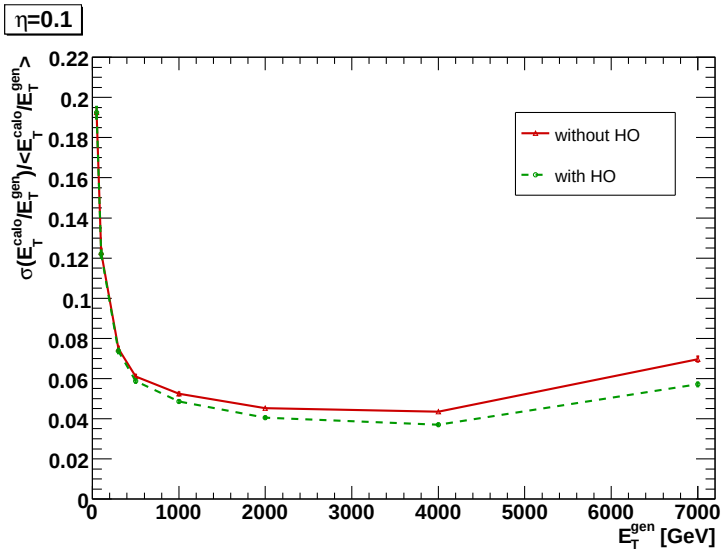

Figure 7: Jet E_{T} resolution as a function of GenJet tranverse energy $E_{\mathrm{T}}^{\mathrm{gen}}$ for parton $\eta = 0.1$.

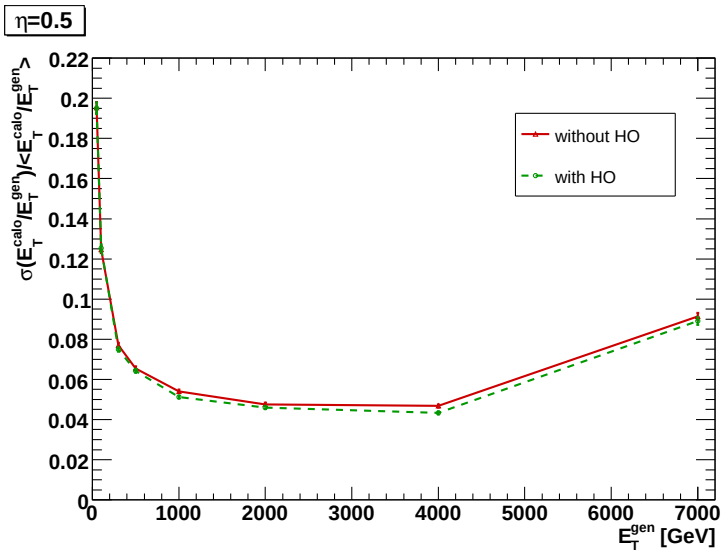

Figure 8: Jet E_{T} resolution as a function of GenJet tranverse energy $E_{\mathrm{T}}^{\mathrm{gen}}$ for parton $\eta = 0.5$.

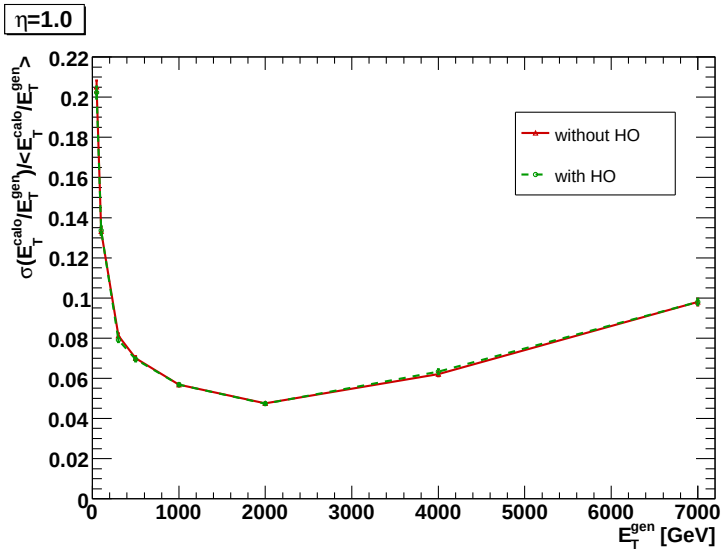

Figure 9: Jet E_{T} resolution as a function of GenJet tranverse energy $E_{\mathrm{T}}^{\mathrm{gen}}$ for parton $\eta = 1.0$.

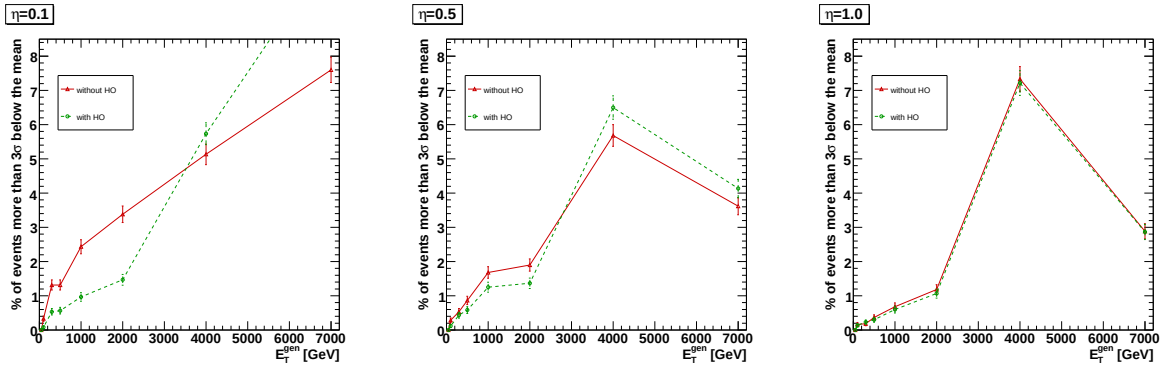

Figure 10: Fraction of events with $E_{\mathrm{T}}^{\mathrm{calo}}/E_{\mathrm{T}}^{\mathrm{gen}}$ ($E_{\mathrm{T}}^{\mathrm{calo,\,HO}}/E_{\mathrm{T}}^{\mathrm{gen}}$) more than 3σ below the mean as a function of GenJet tranverse energy $E_{\mathrm{T}}^{\mathrm{gen}}$ for parton $\eta = 0.1$ (left), 0.5 (center), and 1.0 (right).

4 Summary

A study of impact that HO has on jet reconstruction has been presented. Of particular interest are TeV jets where considerable amount of jet energy can leak outside HB. If HO is used in jet reconstruction, such energy leakages are taken into account and added to the total jet energy. This then improves accuracy of the jet energy measurements as well as measurements of the missing transverse energy.

Starting from CMSSW_2_1_8 HO has been removed from the default jet reconstruction sequence to avoid introducing too much electronics noise into jet energy reconstruction. Main focus of this study was to compare jets reconstructed with and without HO contribution included. Obtained results show small improvements in jet transverse energy resolution when HO is included, especially in the most central η region where Ring 0 is located. However, overall improvement in jet transverse energy resolution is relatively small and it does not exceed 1%. Similarly, when HO is used, effects of energy leakage get reduced, especially in the most central η region.

Finally, it can be concluded that the impact of HO on jet reconstruction is most significant in the most central η region where the effective thickness of the hadronic calorimeter is at its minimum and HB cannot efficiently contain all the energy of very energetic jets. Further out in η space, however, HB has sufficient thickness to efficiently contain even the most energetic jets. Therefore, it is more important to include in jet reconstruction those HO rings that are more central (Ring 0 and Rings ± 1) than those that are further out in η (Rings ± 2).

A Kinematic Distributions for GenJets and CaloJets

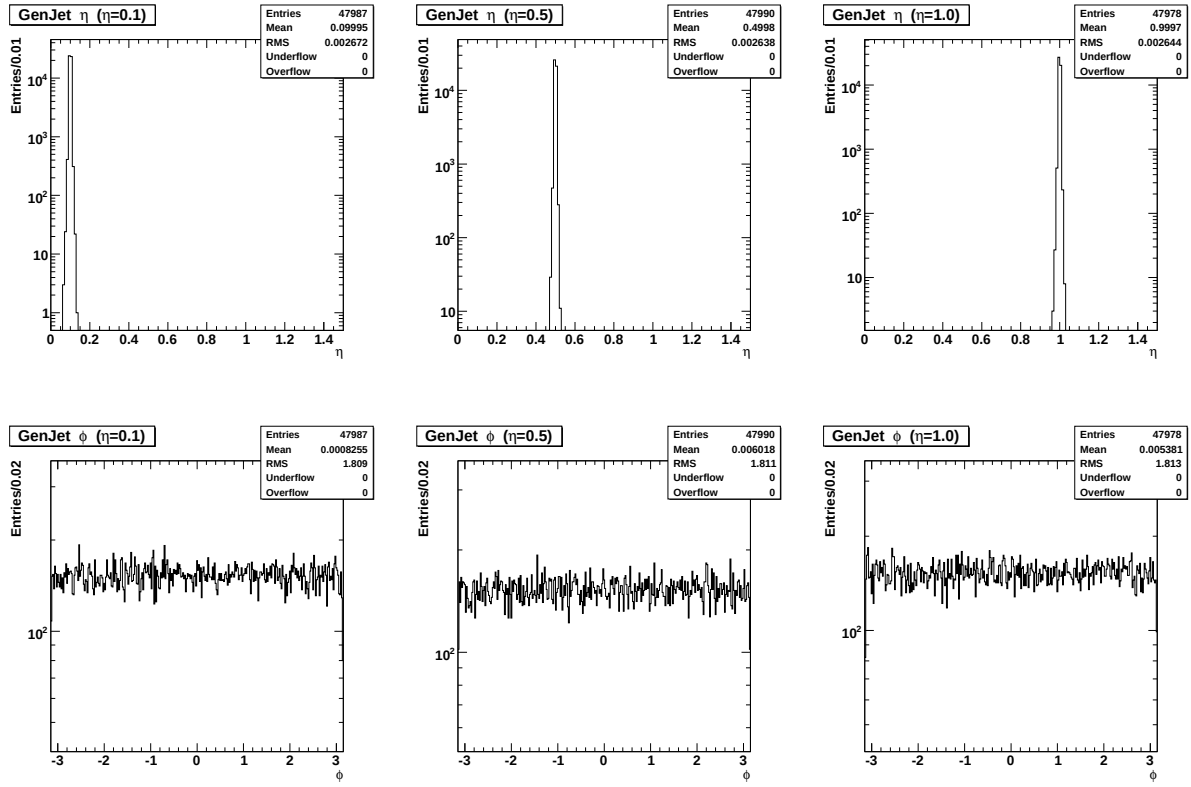

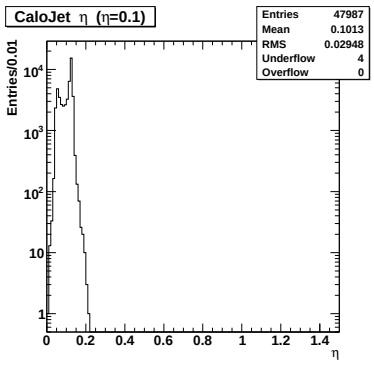
CaloJet η (η=0.1)
Entries 47987
Mean 0.1013
RMS 0.02948
Underflow 4
Overflow 0
Entries/0.01
η

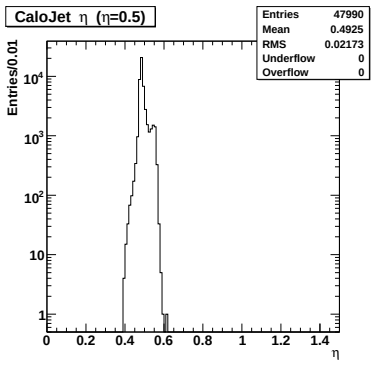
CaloJet η (η=0.5)
Entries 47990
Mean 0.4925
RMS 0.02173
Underflow 0
Overflow 0
Entries/0.01
η

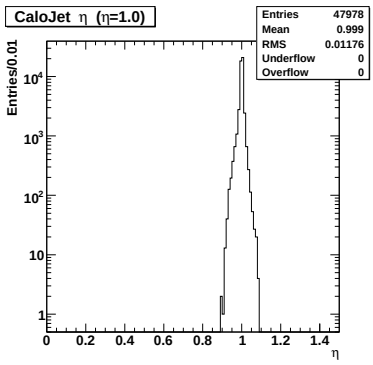
CaloJet η (η=1.0)
Entries 47978
Mean 0.999
RMS 0.01176
Underflow 0
Overflow 0
Entries/0.01
η

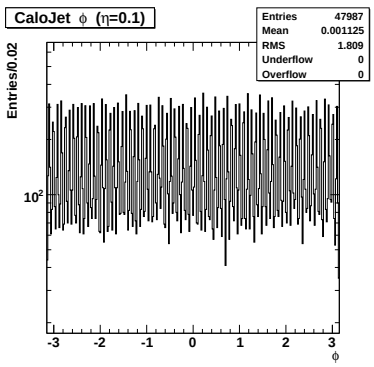
CaloJet ϕ (η=0.1)
Entries 47987
Mean 0.001125
RMS 1.809
Underflow 0
Overflow 0
Entries/0.02
ϕ

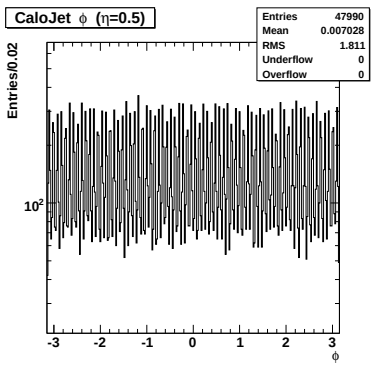
CaloJet ϕ (η=0.5)
Entries 47990
Mean 0.007028
RMS 1.811
Underflow 0
Overflow 0
Entries/0.02
ϕ

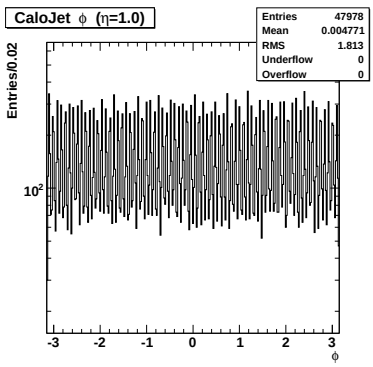
CaloJet ϕ (η=1.0)
Entries 47978
Mean 0.004771
RMS 1.813
Underflow 0
Overflow 0
Entries/0.02
ϕ

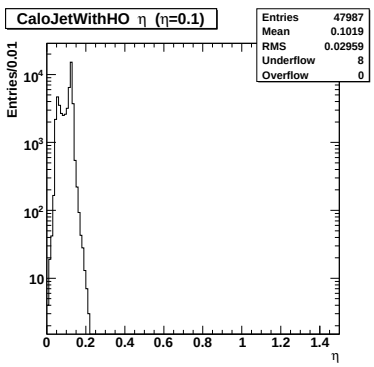
CaloJetWithHO η (η=0.1)
Entries 47987
Mean 0.1019
RMS 0.02959
Underflow 8
Overflow 0
Entries/0.01
η

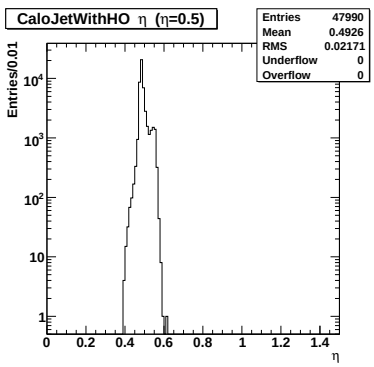
CaloJetWithHO η (η=0.5)
Entries 47990
Mean 0.4926
RMS 0.02171
Underflow 0
Overflow 0
Entries/0.01
η

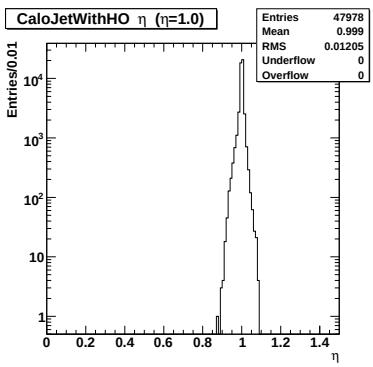
CaloJetWithHO η (η=1.0)
Entries 47978
Mean 0.999
RMS 0.01205
Underflow 0
Overflow 0
Entries/0.01
η

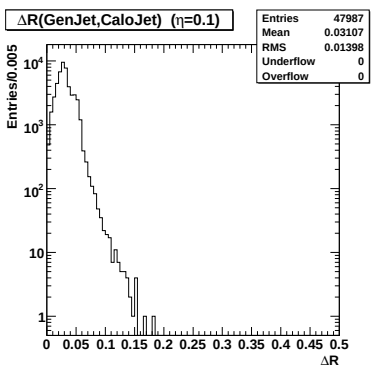
ΔR(GenJet,CaloJet) (η=0.1)
Entries 47987
Mean 0.03107
RMS 0.01398
Underflow 0
Overflow 0
Entries/0.005
ΔR

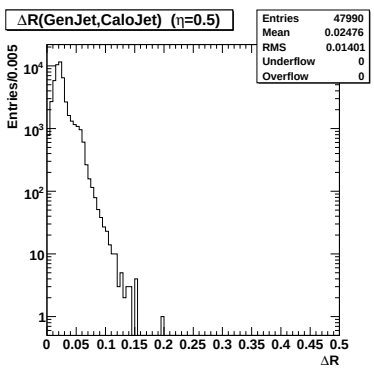
ΔR(GenJet,CaloJet) (η=0.5)
Entries 47990
Mean 0.02476
RMS 0.01401
Underflow 0
Overflow 0
Entries/0.005
ΔR

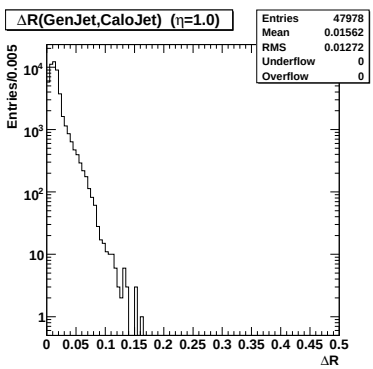
ΔR(GenJet,CaloJet) (η=1.0)
Entries 47978
Mean 0.01562
RMS 0.01272
Underflow 0
Overflow 0
Entries/0.005
ΔR

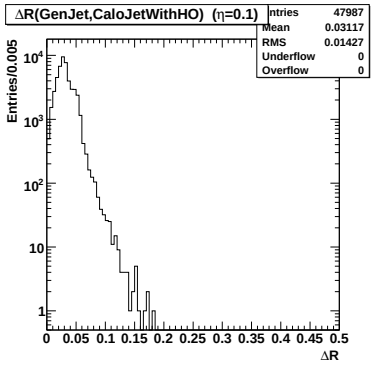

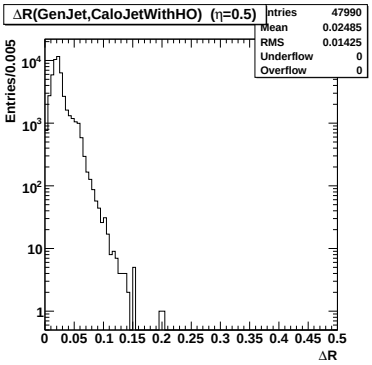

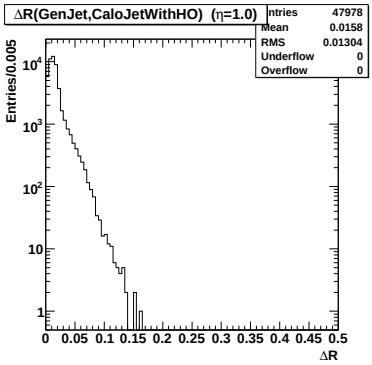

B p_{T} Spectra of the GenJet Constituent Particles

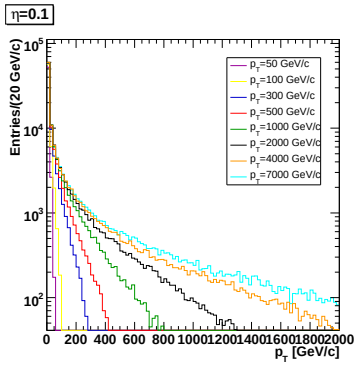

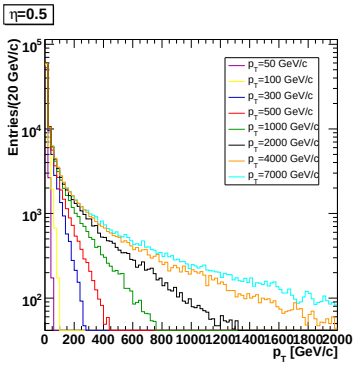

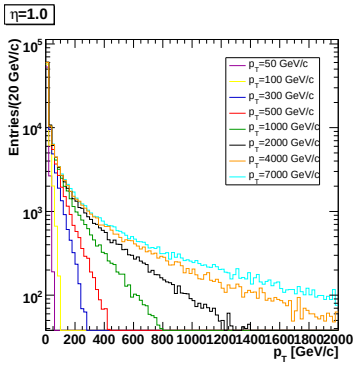

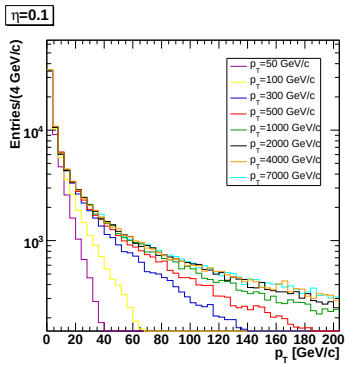

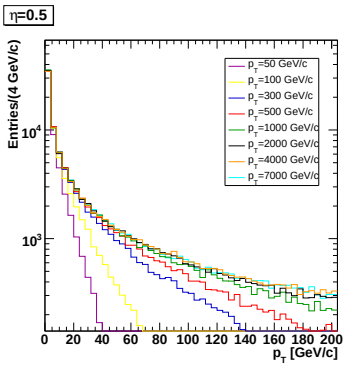

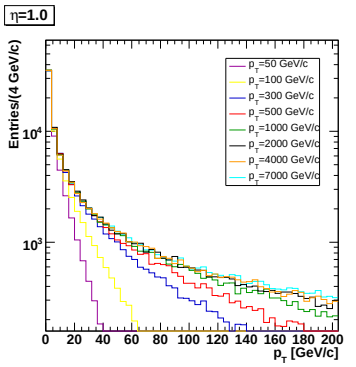

C Gaussian Fits

C.1 CaloJets

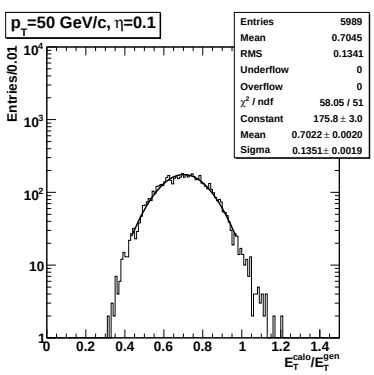

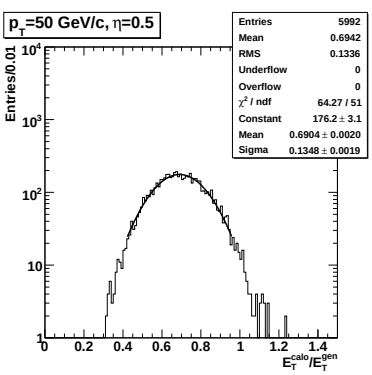

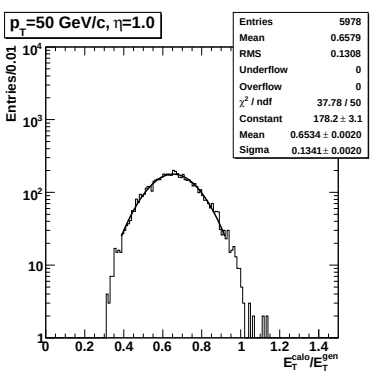

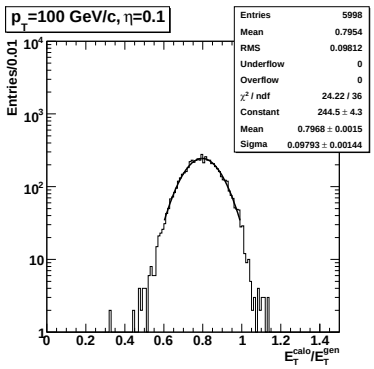
p_T=100 GeV/c, η=0.1
Entries 5998
Mean 0.7954
RMS 0.09812
Underflow 0
Overflow 0
χ² / ndf 24.22 / 36
Constant 244.5 ± 4.3
Mean 0.7968 ± 0.0015
Sigma 0.09793 ± 0.00144
Entries/0.01
E_T^{calo}/E_T^{gen}

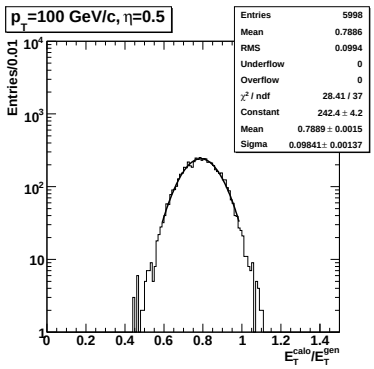
p_T=100 GeV/c, η=0.5
Entries 5998
Mean 0.7886
RMS 0.0994
Underflow 0
Overflow 0
χ² / ndf 28.41 / 37
Constant 242.4 ± 4.2
Mean 0.7889 ± 0.0015
Sigma 0.09841 ± 0.00137
Entries/0.01
E_T^{calo}/E_T^{gen}

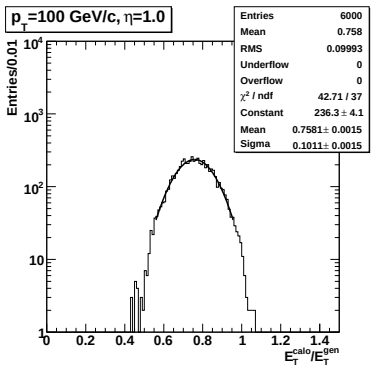
p_T=100 GeV/c, η=1.0
Entries 6000
Mean 0.758
RMS 0.09993
Underflow 0
Overflow 0
χ² / ndf 42.71 / 37
Constant 236.3 ± 4.1
Mean 0.7581 ± 0.0015
Sigma 0.1011 ± 0.0015
Entries/0.01
E_T^{calo}/E_T^{gen}

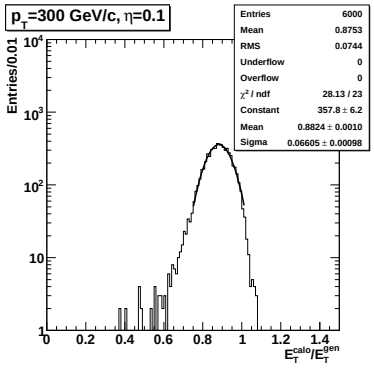
p_T=300 GeV/c, η=0.1
Entries 6000
Mean 0.8753
RMS 0.0744
Underflow 0
Overflow 0
χ² / ndf 28.13 / 23
Constant 357.8 ± 6.2
Mean 0.8824 ± 0.0010
Sigma 0.06605 ± 0.00098
Entries/0.01
E_T^{calo}/E_T^{gen}

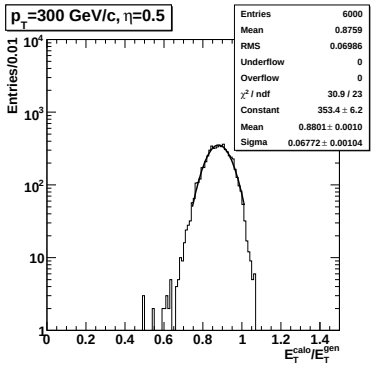
p_T=300 GeV/c, η=0.5
Entries 6000
Mean 0.8759
RMS 0.06986
Underflow 0
Overflow 0
χ² / ndf 30.9 / 23
Constant 353.4 ± 6.2
Mean 0.8801 ± 0.0010
Sigma 0.06772 ± 0.00104
Entries/0.01
E_T^{calo}/E_T^{gen}

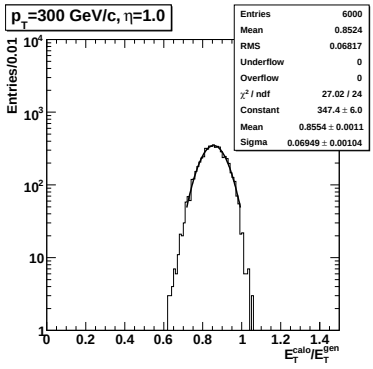
p_T=300 GeV/c, η=1.0
Entries 6000
Mean 0.8524
RMS 0.06817
Underflow 0
Overflow 0
χ² / ndf 27.02 / 24
Constant 347.4 ± 6.0
Mean 0.8554 ± 0.0011
Sigma 0.06949 ± 0.00104
Entries/0.01
E_T^{calo}/E_T^{gen}

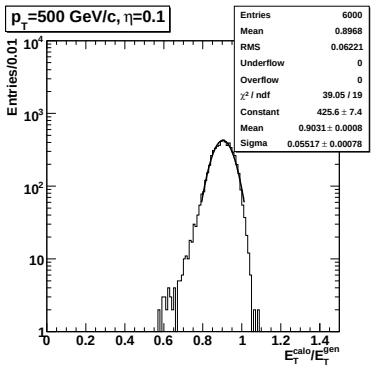
p_T=500 GeV/c, η=0.1
Entries 6000
Mean 0.8968
RMS 0.06221
Underflow 0
Overflow 0
χ² / ndf 39.05 / 19
Constant 425.6 ± 7.4
Mean 0.9031 ± 0.0008
Sigma 0.05517 ± 0.00078
Entries/0.01
E_T^{calo}/E_T^{gen}

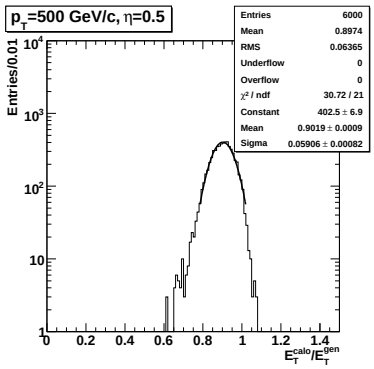
p_T=500 GeV/c, η=0.5
Entries 6000
Mean 0.8974
RMS 0.06365
Underflow 0
Overflow 0
χ² / ndf 30.72 / 21
Constant 402.5 ± 6.9
Mean 0.9019 ± 0.0009
Sigma 0.05906 ± 0.00082
Entries/0.01
E_T^{calo}/E_T^{gen}

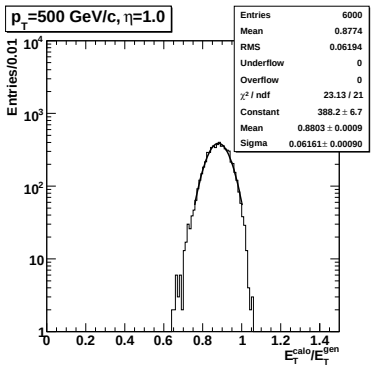
p_T=500 GeV/c, η=1.0
Entries 6000
Mean 0.8774
RMS 0.06194
Underflow 0
Overflow 0
χ² / ndf 23.13 / 21
Constant 388.2 ± 6.7
Mean 0.8803 ± 0.0009
Sigma 0.06161 ± 0.00090
Entries/0.01
E_T^{calo}/E_T^{gen}

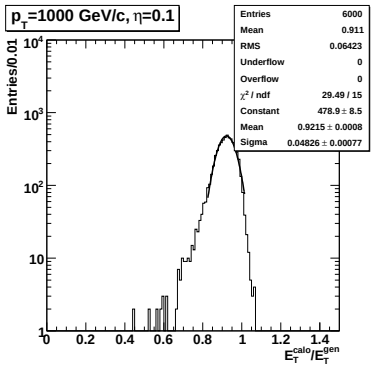
p_T=1000 GeV/c, η=0.1
Entries 6000
Mean 0.911
RMS 0.06423
Underflow 0
Overflow 0
χ² / ndf 29.49 / 15
Constant 478.9 ± 8.5
Mean 0.9215 ± 0.0008
Sigma 0.04826 ± 0.00077
Entries/0.01
E_T^{calo}/E_T^{gen}

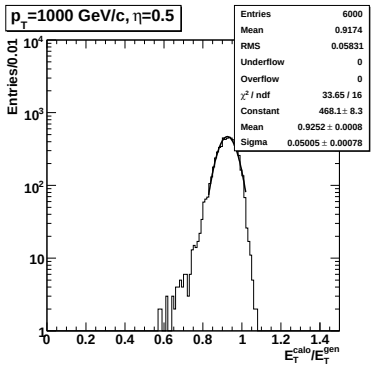
p_T=1000 GeV/c, η=0.5
Entries 6000
Mean 0.9174
RMS 0.05831
Underflow 0
Overflow 0
χ² / ndf 33.65 / 16
Constant 468.1 ± 8.3
Mean 0.9252 ± 0.0008
Sigma 0.05005 ± 0.00078
Entries/0.01
E_T^{calo}/E_T^{gen}

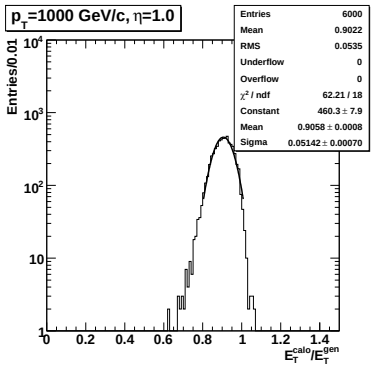
p_T=1000 GeV/c, η=1.0
Entries 6000
Mean 0.9022
RMS 0.0535
Underflow 0
Overflow 0
χ² / ndf 62.21 / 18
Constant 460.3 ± 7.9
Mean 0.9058 ± 0.0008
Sigma 0.05142 ± 0.00070
Entries/0.01
E_T^{calo}/E_T^{gen}

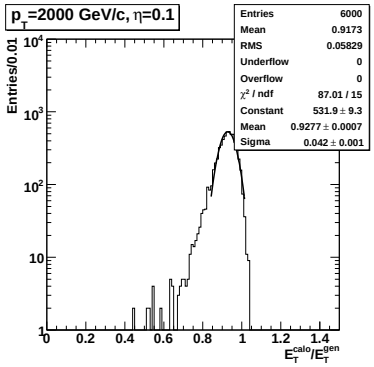

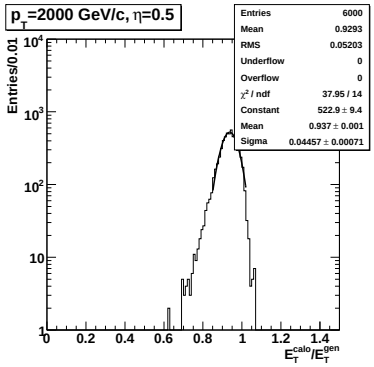

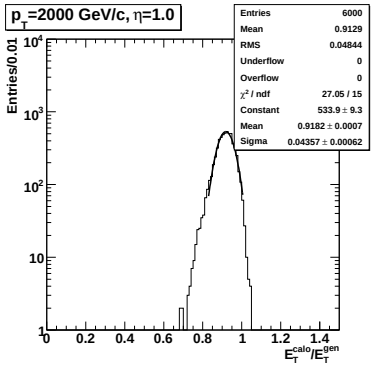

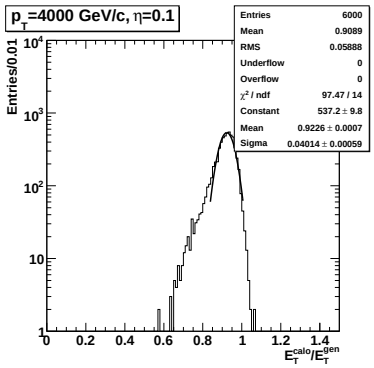

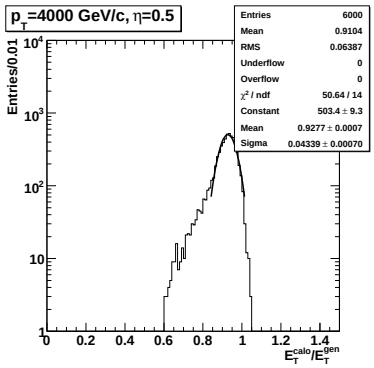

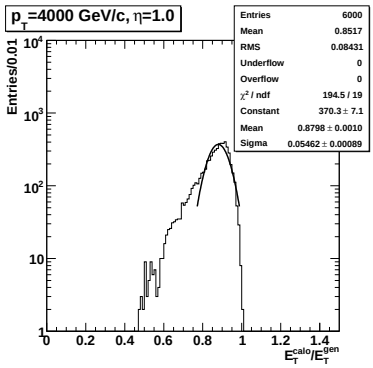

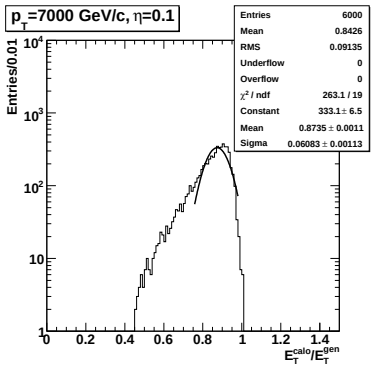

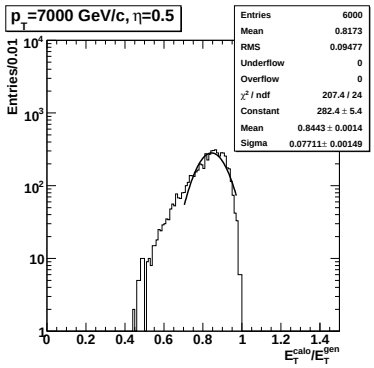

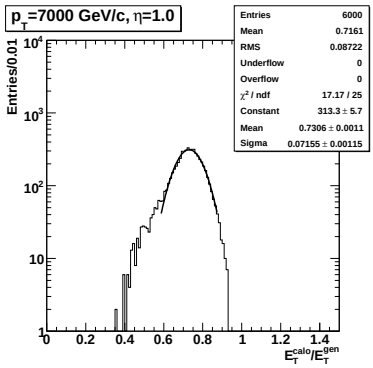

C.2 CaloJetsWithHO

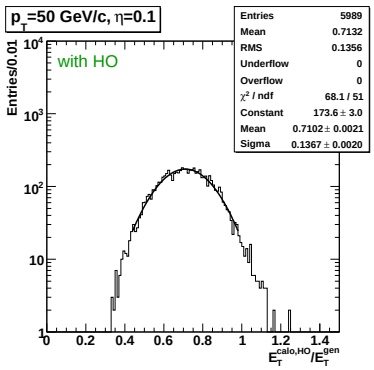

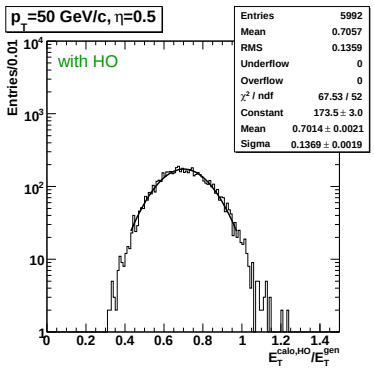

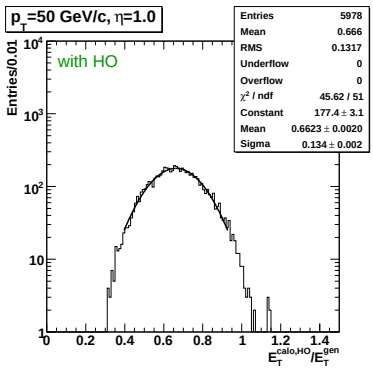

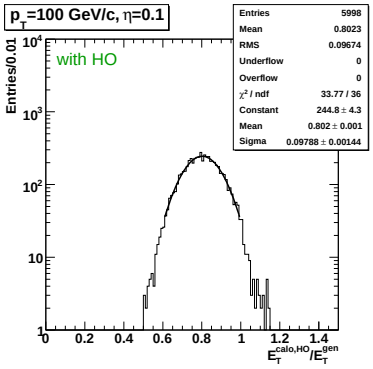
p_T=100 GeV/c, η=0.1
with HO
Entries 5998
Mean 0.8023
RMS 0.09674
Underflow 0
Overflow 0
χ² / ndf 33.77 / 36
Constant 244.8 ± 4.3
Mean 0.802 ± 0.001
Sigma 0.09788 ± 0.00144
Entries/0.01
E_T^calo,HO/E_T^gen

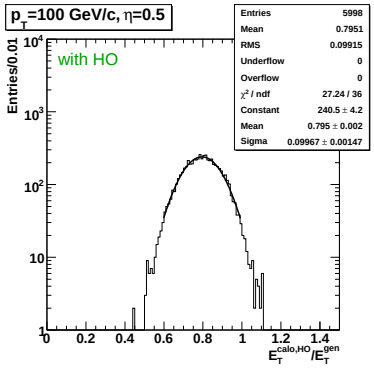
p_T=100 GeV/c, η=0.5
with HO
Entries 5998
Mean 0.7951
RMS 0.09915
Underflow 0
Overflow 0
χ² / ndf 27.24 / 36
Constant 240.5 ± 4.2
Mean 0.795 ± 0.002
Sigma 0.09967 ± 0.00147
Entries/0.01
E_T^calo,HO/E_T^gen

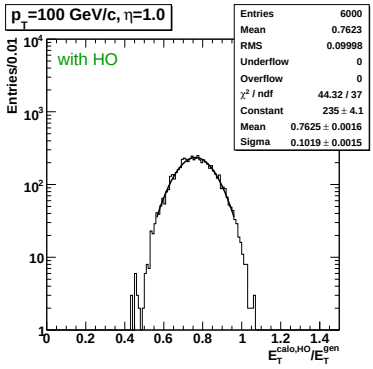
p_T=100 GeV/c, η=1.0
with HO
Entries 6000
Mean 0.7623
RMS 0.09998
Underflow 0
Overflow 0
χ² / ndf 44.32 / 37
Constant 235 ± 4.1
Mean 0.7625 ± 0.0016
Sigma 0.1019 ± 0.0015
Entries/0.01
E_T^calo,HO/E_T^gen

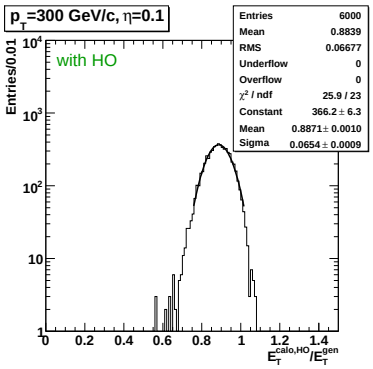
p_T=300 GeV/c, η=0.1
with HO
Entries 6000
Mean 0.8839
RMS 0.06677
Underflow 0
Overflow 0
χ² / ndf 25.9 / 23
Constant 366.2 ± 6.3
Mean 0.8871 ± 0.0010
Sigma 0.0654 ± 0.0009
Entries/0.01
E_T^calo,HO/E_T^gen

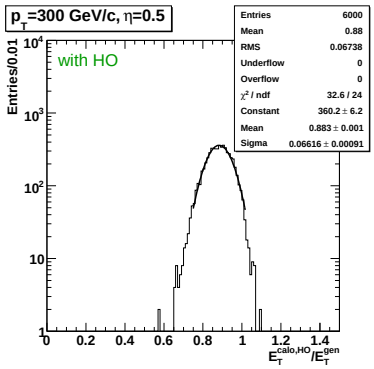
p_T=300 GeV/c, η=0.5
with HO
Entries 6000
Mean 0.88
RMS 0.06738
Underflow 0
Overflow 0
χ² / ndf 32.6 / 24
Constant 360.2 ± 6.2
Mean 0.883 ± 0.001
Sigma 0.06616 ± 0.00091
Entries/0.01
E_T^calo,HO/E_T^gen

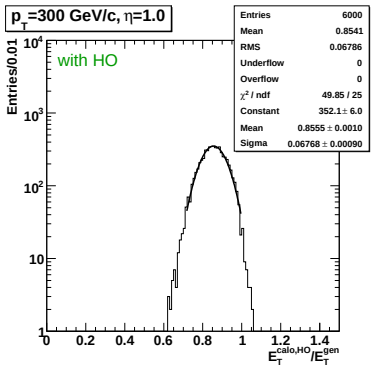
p_T=300 GeV/c, η=1.0
with HO
Entries 6000
Mean 0.8541
RMS 0.06786
Underflow 0
Overflow 0
χ² / ndf 49.85 / 25
Constant 352.1 ± 6.0
Mean 0.8555 ± 0.0010
Sigma 0.06768 ± 0.00090
Entries/0.01
E_T^calo,HO/E_T^gen

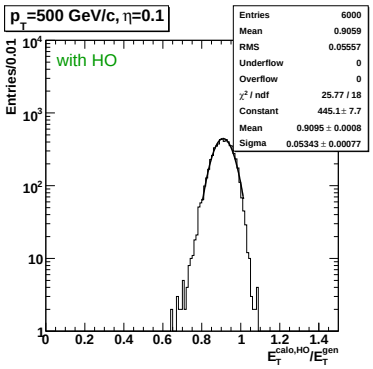
p_T=500 GeV/c, η=0.1
with HO
Entries 6000
Mean 0.9059
RMS 0.05557
Underflow 0
Overflow 0
χ² / ndf 25.77 / 18
Constant 445.1 ± 7.7
Mean 0.9095 ± 0.0008
Sigma 0.05343 ± 0.00077
Entries/0.01
E_T^calo,HO/E_T^gen

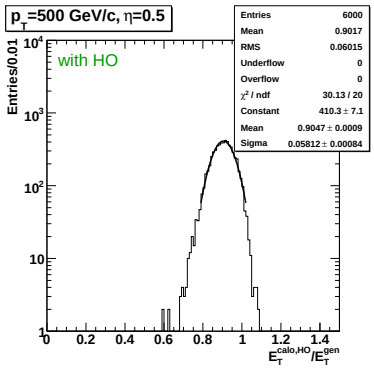
p_T=500 GeV/c, η=0.5
with HO
Entries 6000
Mean 0.9017
RMS 0.06015
Underflow 0
Overflow 0
χ² / ndf 30.13 / 20
Constant 410.3 ± 7.1
Mean 0.9047 ± 0.0009
Sigma 0.05812 ± 0.00084
Entries/0.01
E_T^calo,HO/E_T^gen

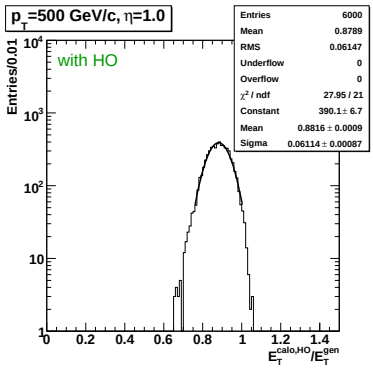
p_T=500 GeV/c, η=1.0
with HO
Entries 6000
Mean 0.8789
RMS 0.06147
Underflow 0
Overflow 0
χ² / ndf 27.95 / 21
Constant 390.1 ± 6.7
Mean 0.8816 ± 0.0009
Sigma 0.06114 ± 0.00087
Entries/0.01
E_T^calo,HO/E_T^gen

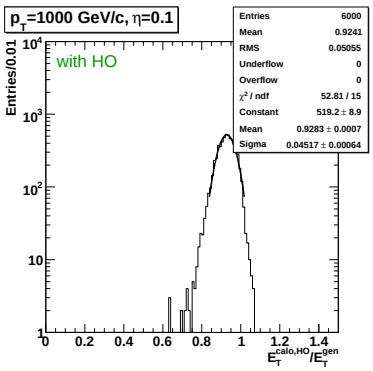
p_T=1000 GeV/c, η=0.1
with HO
Entries 6000
Mean 0.9241
RMS 0.05055
Underflow 0
Overflow 0
χ² / ndf 52.81 / 15
Constant 519.2 ± 8.9
Mean 0.9283 ± 0.0007
Sigma 0.04517 ± 0.00064
Entries/0.01
E_T^calo,HO/E_T^gen

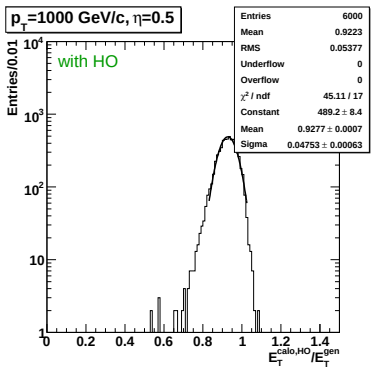
p_T=1000 GeV/c, η=0.5
with HO
Entries 6000
Mean 0.9223
RMS 0.05377
Underflow 0
Overflow 0
χ² / ndf 45.11 / 17
Constant 489.2 ± 8.4
Mean 0.9277 ± 0.0007
Sigma 0.04753 ± 0.00063
Entries/0.01
E_T^calo,HO/E_T^gen

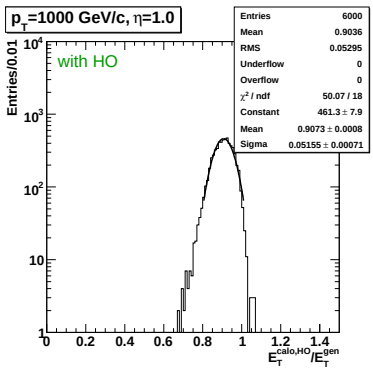
p_T=1000 GeV/c, η=1.0
with HO
Entries 6000
Mean 0.9036
RMS 0.05295
Underflow 0
Overflow 0
χ² / ndf 50.07 / 18
Constant 461.3 ± 7.9
Mean 0.9073 ± 0.0008
Sigma 0.05155 ± 0.00071
Entries/0.01
E_T^calo,HO/E_T^gen

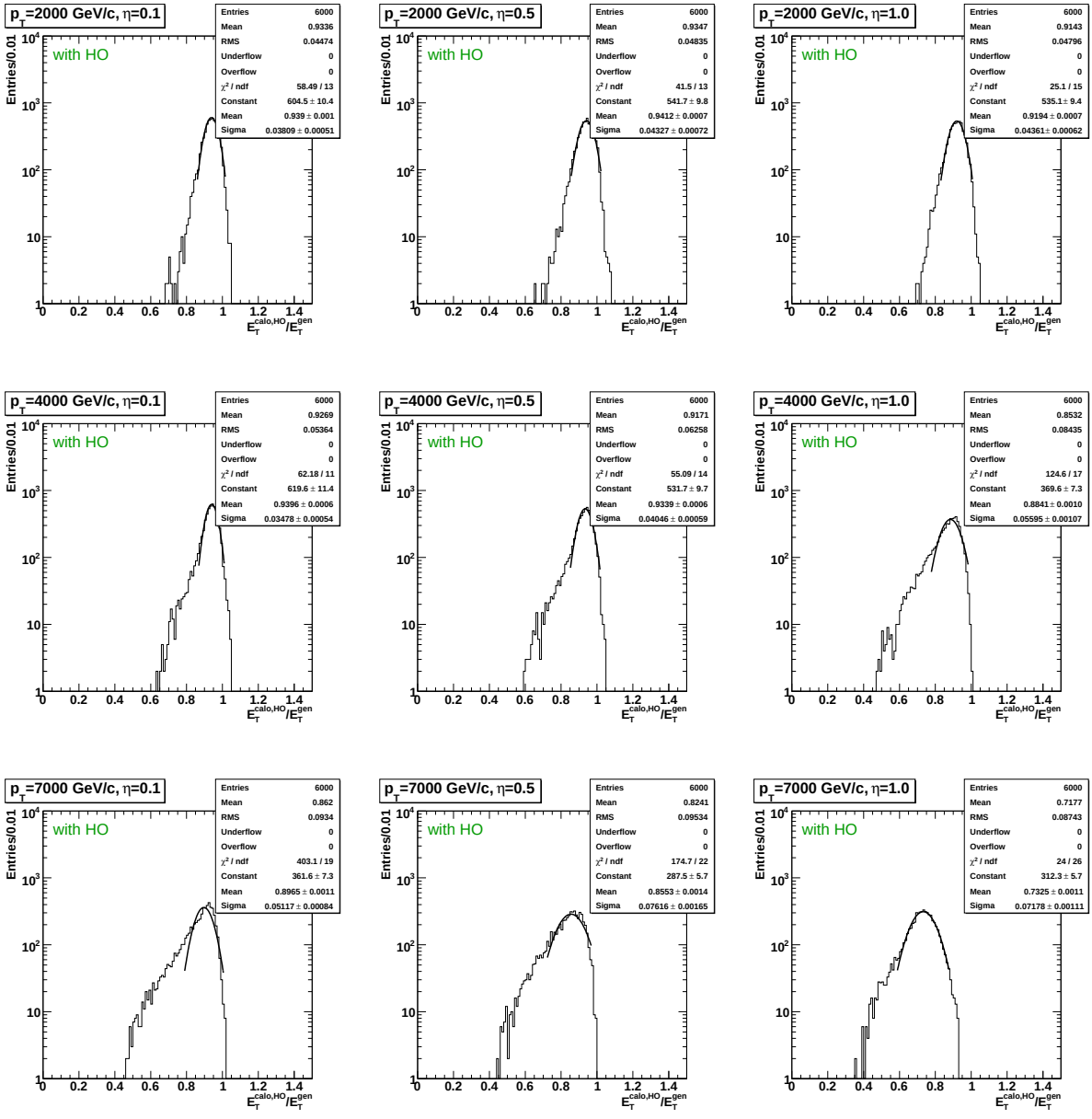

D Jet E_{T} Resolution vs. `hadEnergyInHO` Weight Factor

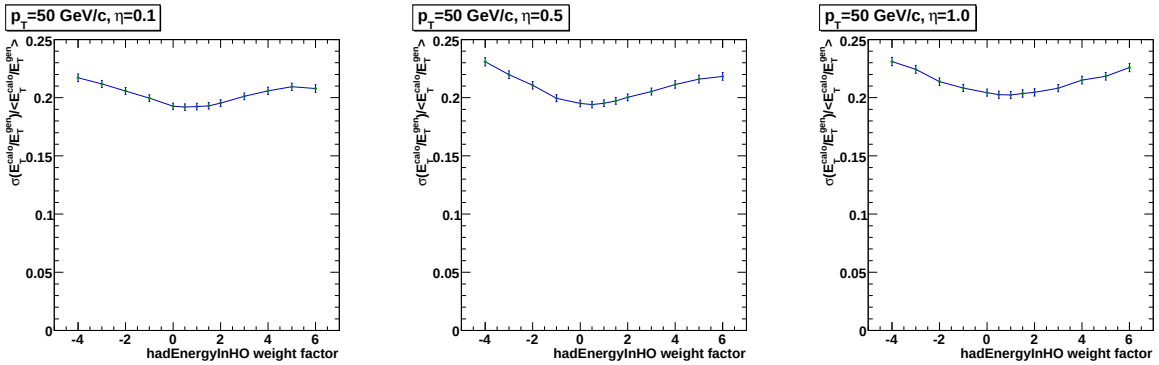

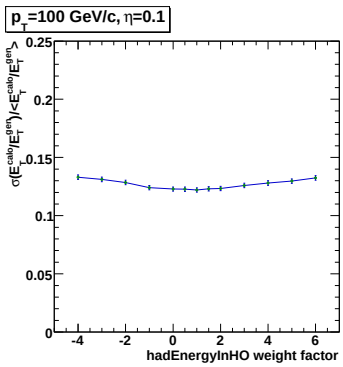
p_T=100 GeV/c, η=0.1
σ(E_T^calo/E_T^gen)/<E_T^calo/E_T^gen>
hadEnergyInHO weight factor

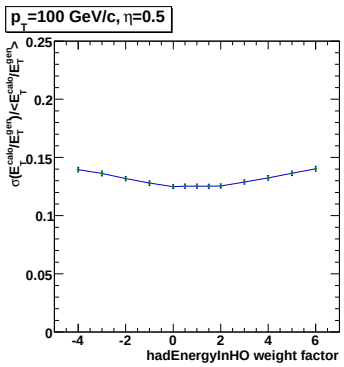
p_T=100 GeV/c, η=0.5
σ(E_T^calo/E_T^gen)/<E_T^calo/E_T^gen>
hadEnergyInHO weight factor

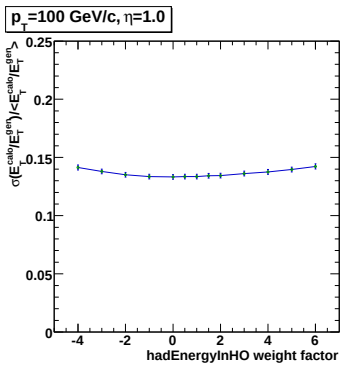
p_T=100 GeV/c, η=1.0
σ(E_T^calo/E_T^gen)/<E_T^calo/E_T^gen>
hadEnergyInHO weight factor

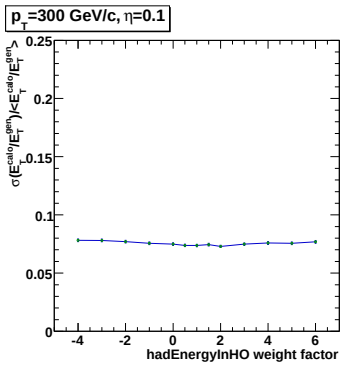
p_T=300 GeV/c, η=0.1
σ(E_T^calo/E_T^gen)/<E_T^calo/E_T^gen>
hadEnergyInHO weight factor

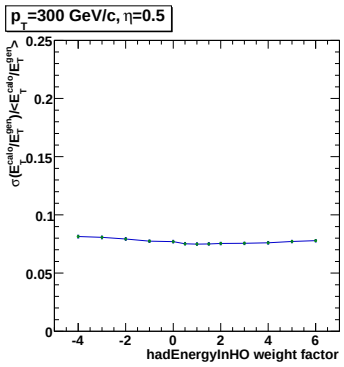
p_T=300 GeV/c, η=0.5
σ(E_T^calo/E_T^gen)/<E_T^calo/E_T^gen>
hadEnergyInHO weight factor

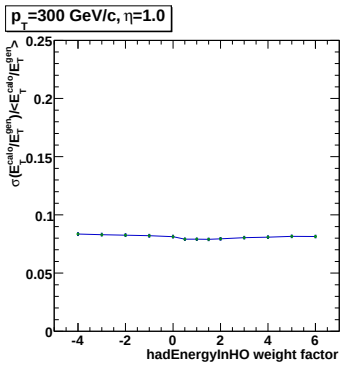
p_T=300 GeV/c, η=1.0
σ(E_T^calo/E_T^gen)/<E_T^calo/E_T^gen>
hadEnergyInHO weight factor

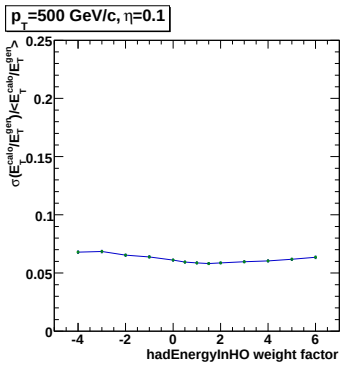
p_T=500 GeV/c, η=0.1
σ(E_T^calo/E_T^gen)/<E_T^calo/E_T^gen>
hadEnergyInHO weight factor

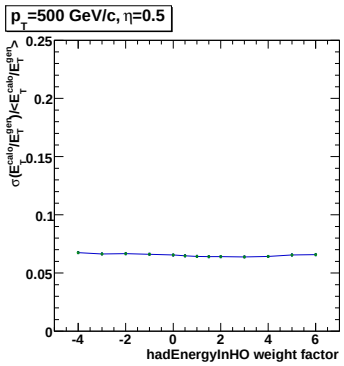
p_T=500 GeV/c, η=0.5
σ(E_T^calo/E_T^gen)/<E_T^calo/E_T^gen>
hadEnergyInHO weight factor

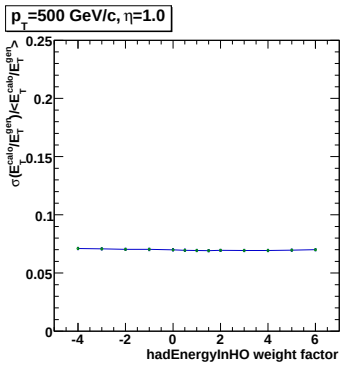
p_T=500 GeV/c, η=1.0
σ(E_T^calo/E_T^gen)/<E_T^calo/E_T^gen>
hadEnergyInHO weight factor

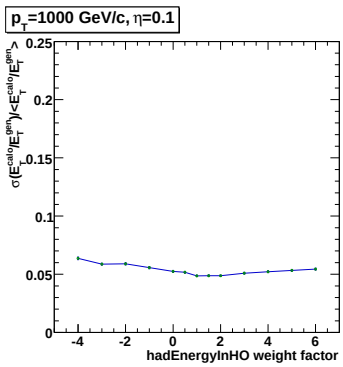
p_T=1000 GeV/c, η=0.1
σ(E_T^calo/E_T^gen)/<E_T^calo/E_T^gen>
hadEnergyInHO weight factor

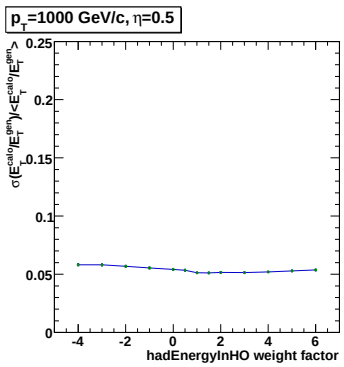
p_T=1000 GeV/c, η=0.5
σ(E_T^calo/E_T^gen)/<E_T^calo/E_T^gen>
hadEnergyInHO weight factor

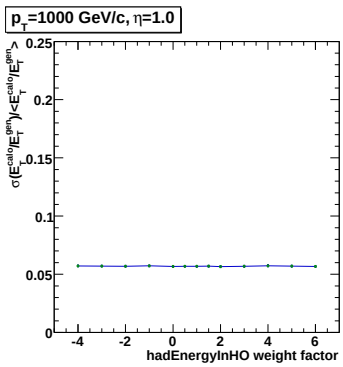
p_T=1000 GeV/c, η=1.0
σ(E_T^calo/E_T^gen)/<E_T^calo/E_T^gen>
hadEnergyInHO weight factor

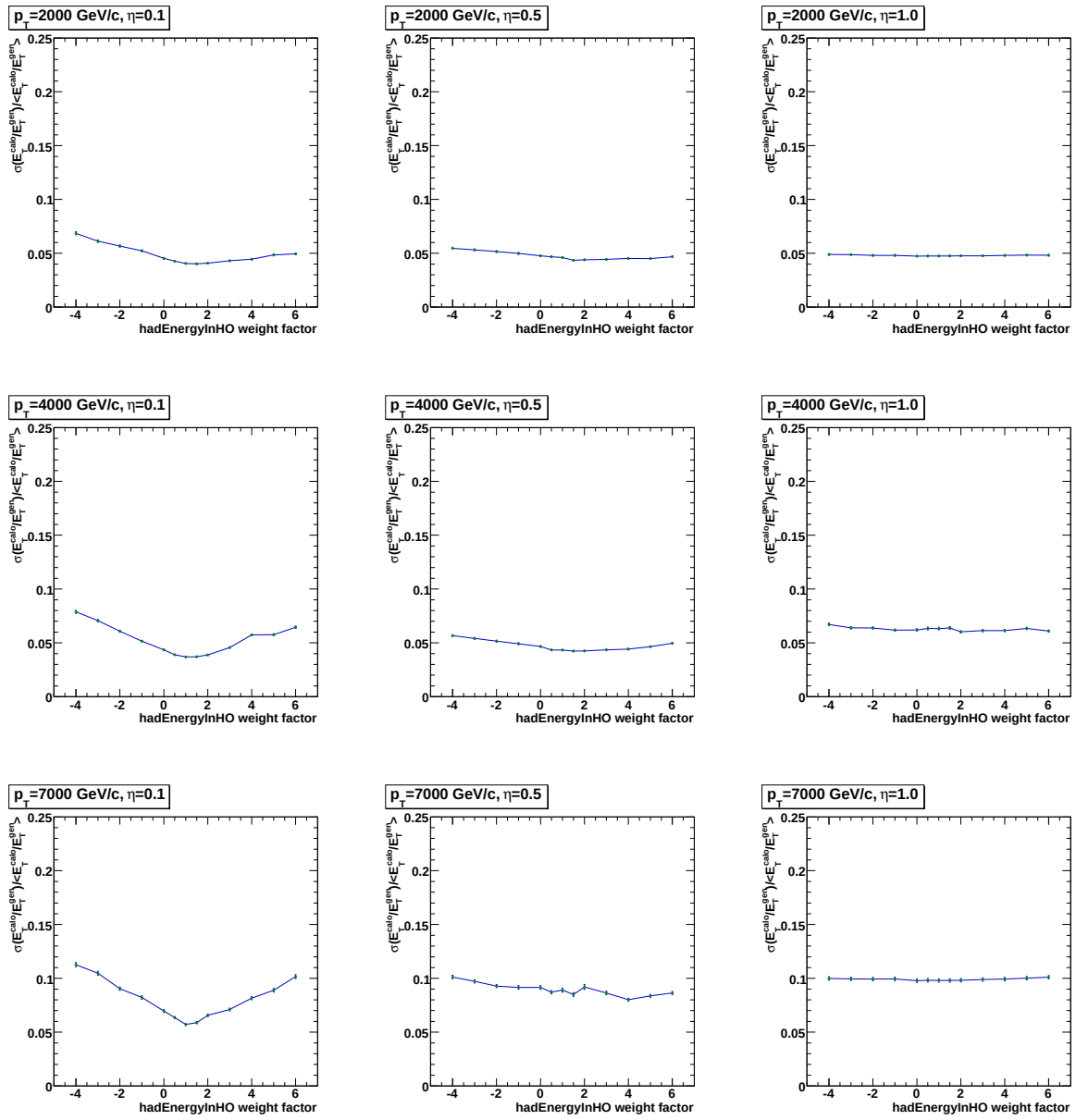

References

[1] The CMS Collaboration, S. Chatrchyan *et al.*, "The CMS Experiment at the CERN LHC", 2008 JINST **3** S08004

[2] Global Tags for Conditions Data: https://twiki.cern.ch/twiki/bin/view/CMS/SWGuideFrontierConditions

[3] CMSSW Application Framework: https://twiki.cern.ch/twiki/bin/view/CMS/WorkBookCMSSWFramework

[4] R. Demina *et al.*, "Calorimeter Cell Energy Thresholds for Jet Reconstruction in CMS", CMS NOTE 2006/020

[5] Z. Qi *et al.*, "HCAL Noise Thresholds in CMSSW_2_2_3", Jet Algorithms Meeting, Jan 15, 2009 http://indico.cern.ch/getFile.py/access?contribId=1&resId=1&materialId=slides&confId=49768

[6] C. Sander *et al.*, "$\not\!\!E_{\rm T}$ from Simulated Very High $p_{\rm T}$ Jets", MET Working Group Meeting, Nov 21, 2008 http://indico.cern.ch/getFile.py/access?contribId=2&resId=0&materialId=slides&confId=45919

[7] One-To-One Matching Tool: https://twiki.cern.ch/twiki/bin/view/CMS/WorkBookJetAnalysis